

2. *Faulting of the Great Kanto Earthquake of 1923 as Revealed by Seismological Data.*

By Hiroo KANAMORI,

Earthquake Research Institute.

(Read September 22, 1970.—Received September 24, 1970.)

Abstract

The fault parameters of the Great Kanto earthquake of September 1, 1923, are determined on the basis of the first-motion data, aftershock area, and the amplitude of surface waves at teleseismic stations. It is found that the faulting of this earthquake is a reverse right-lateral fault on a plane which dips 34° towards $N20^\circ E$. The auxiliary plane has a dip of 80° towards $S55^\circ E$. This means that the foot-wall side moves approximately north-west with respect to the hanging wall side. The strike of the fault plane is almost parallel to that of the Sagami trough, and the slip direction is more or less perpendicular to the trend of the Japan trench. This earthquake is therefore considered to represent a slippage between two crustal blocks bounded by the Sagami trough. A seismic moment of 7.6×10^{27} dyne-cm is obtained. If the fault dimension is taken to be 130×70 km², the average slip on the fault plane and the stress drop are estimated to be 2.1 m and 18 bars respectively. This slip is about 1/3 of that estimated from geodetic data. This discrepancy may indicate an existence of a pre-seismic deformation which did not contribute to the seismic wave radiation, but the evidence from other observations is not very firm.

This paper which represents an extension of the earlier paper by *Kanamori and Miyamura* (1970) discusses a possible mode of faulting associated with the Great Kanto earthquake of Sept. 1, 1923.

The data used in the present analysis are: (1) relocated hypocenters of the main shock and the largest aftershock; (2) the first motions of *P* waves recorded at Japanese stations and at several teleseismic stations; (3) the amplitude of long-period (80 sec) Love and Rayleigh waves. The first motions of *P* waves at Japanese stations were reported by *Nakamura* (1925). In order to supplement these data we read the seismograms at Berkeley, Wien, Uppsala, Zagreb, and Riverview. In plotting the first-motion data on the Wulff grid one problem arises. The angle of emergence *i* of the ray leaving the focus for nearby stations is greatly affected by the depth of the source and the crustal structure. Fortunately the depth of this earthquake is constrained fairly well by the *P* times at nearby stations; *Kanamori and Miyamura* (1970) concluded

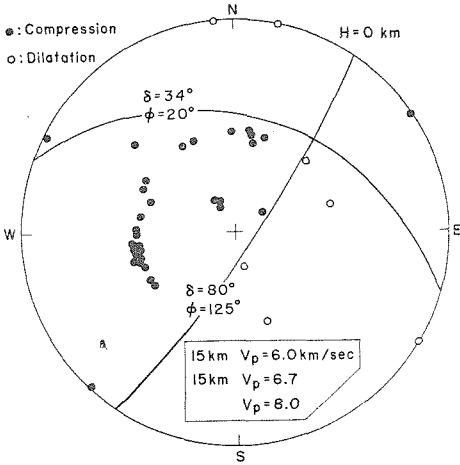


Fig. 1. Stereographic projection of the lower half of the focal sphere. The focal depth is assumed to be 0 km. δ is the dip angle and ϕ is the dip direction. The insert shows the crustal structure used for the calculation of the emergence angle of the ray leaving the focus.

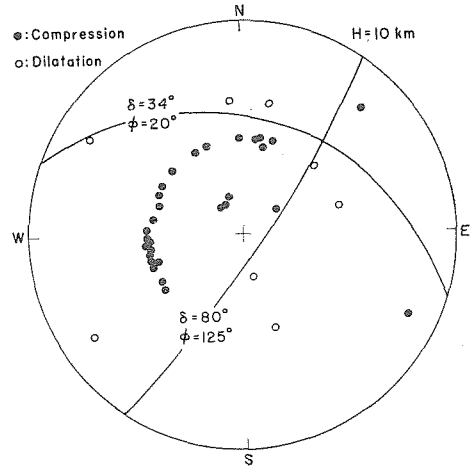


Fig. 2. Stereographic projection of the lower half of the focal sphere. The focal depth is assumed to be 10 km. δ is the dip angle and ϕ is the dip direction.

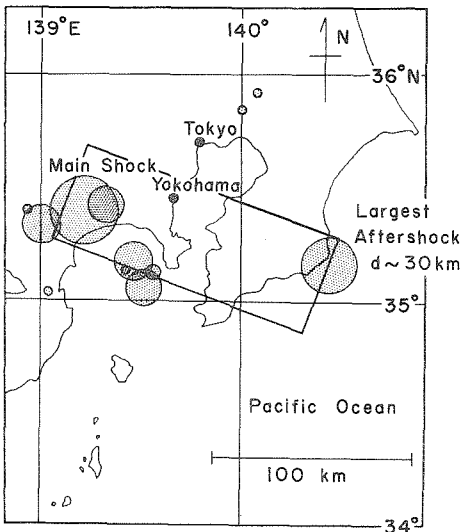


Fig. 3. Major aftershocks (dotted circle) which occurred within 24 hours after the main shock. The size of the circle is approximately proportional to the size of each shock.

that the initial break of this earthquake occurred in the crust not deeper than 10 km. We therefore computed i for the depth of 0 and 10 km, using a two-layered crustal structure as shown in the insert of Figure 1. This structure is probably appropriate for the present purpose. The first-motion data were then plotted on the Wulff grid and are shown in Figures 1 and 2 for the depths of 0 and 10 km respectively. Although the distributions of compressions and dilatations differ for the two cases, the fault plane solutions are almost identical as shown in Figures 1 and 2. The nodal planes are constrained reasonably well, though they are not completely free from ambiguity. One nodal plane has a dip angle of 34° and dip direction of $N20^\circ E$, and the

Another nodal plane has a dip angle of 80° and dip direction of $N125^\circ E$.

other has a dip angle of 80° and dip direction of $S55^\circ E$. Which of these nodal planes represents the actual fault plane cannot be determined on the basis of the distribution of the first motions alone. The distribution of the aftershocks may give a clue to the selection of the fault plane.

Figure 3 shows the epicenters of the mainshock and the aftershocks which occurred within twenty-four hours after the mainshock. All the epicenters except those for the mainshock and the largest aftershock are taken from *Imamura and Hasegawa (1928)*. The epicenter of the mainshock is taken from *Kanamori and Miyamura (1970)*, and the largest aftershock was relocated on the basis of *P*-times recorded at 67 worldwide stations. The method of the relocation is the same as that employed by *Kanamori and Miyamura (1970)*. Unlike the mainshock, a somewhat large depth, 30 km, gave a minimum root-mean-square of *O-C* residuals. This aftershock is by far the largest among all the aftershocks. A comparison of the size of this aftershocks with the mainshock may be made on the seismogram recorded, for example, at Suva, Fiji Islands, as shown in Figure 4. The hypocenter parameters are: origin time Sept. 2, 1923, $02^h46^m42^s$; latitude $35.13^\circ N$; longitude $140.54^\circ E$; depth 30 km. The E-W trending distribution of the larger aftershocks strongly suggests that the nodal plane dipping towards $N20^\circ E$ is the fault plane. Thus we take a plane dipping 34° towards $N20^\circ E$ and having a size comparable to that of the aftershock area as the fault plane of the Kanto earthquake (see Figure 3). This fault represents a reverse right-lateral faulting with a slip angle of the foot-wall side of 18° measured, on the fault plane, from $N70^\circ W$. The deeper focus of the largest aftershock suggests that it occurred also on the major fault plane.

The seismic moment can be determined from the amplitude of long-period surface waves. Love and Rayleigh waves having a period of about 80 sec could be recovered from the seismograms recorded at the stations listed in Table 1. The theoretical amplitude of surface waves for the fault geometry determined above was calculated with the method described by *Kanamori (1971)*. The earth model 5.08 M was

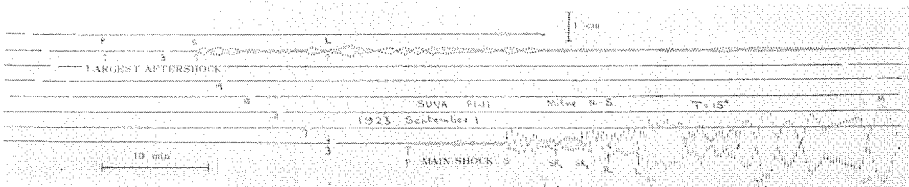


Fig. 4. Seismogram which includes the mainshock and the largest aftershock recorded at Suva, Fiji Islands, by Milne seismograph.

Table 1. Seismic moment determined at a period of 80 sec.

	Distance (degree)	Azimuth (degree)	Com- ponent	Phase	$A_0(f)$ cm sec	$G(f)$ cm sec	M_0 10^{27} dyne- cm
Berkeley	75.17	54	E-W	G_1	7.7	1.0	7.7
Georgetown	98.84	28	E-W	G_1	14.0	1.7	8.2
La Paz	146.93	59	N-S	G_1	5.2	0.74	7.0
Ottawa	93.64	24	E-W	G_1	16.0	1.7	9.4
Wien	82.38	326	UD	R_1	16.0	1.8	8.9
Zagreb	84.32	324	NW-SE	G_1	4.3	1.0	4.3
Average							7.6

used, and a point source was placed at a depth of 16 km, the estimated average depth of the fault. In Table 1 are listed the observed amplitude spectral densities $|A_0(f)|$ corrected for the instrument response, attenuation, and the ray-spreading together with the theoretical spectral densities $|G(f)|$ for a moment of 10^{27} dyne-cm. The ratio $|A_0(f)|/|G(f)|$ gives the seismic moment with the unit of 10^{27} dyne-cm. The values obtained for Love and Rayleigh waves and for stations located at different azimuths agree with one another reasonably well. This result suggests that the fault geometry determined by the first motions is consistent also with the surface-wave radiation. An average moment of $M_0 = 7.6 \times 10^{27}$ dyne-cm is obtained. The average slip dislocation \bar{u} on the fault plane and the stress drop $\Delta\sigma$ can be estimated from the relations $\bar{u} = M_0/Lw\mu$, and $\Delta\sigma = 2\eta\mu\bar{u}/w$ where L is the fault length, w the fault width, μ the rigidity, and η is the geometrical factor. The fault length is fairly well defined by the aftershock area as 130 km, but the width is somewhat uncertain. We assumed $w \sim 70$ km, $\mu \sim 0.4 \times 10^{12}$ dyne-cm, and $\eta = 0.74$ (the average for strike-slip and dip-slip faults) and obtained $\bar{u} \sim 2.1$ m and $\Delta\sigma \sim 18$ bars. Because of the uncertainty in the fault dimension these values may be uncertain by a factor of 2.

An independent study made by Ando (1971) who used geodetic (triangulation and leveling) as well as geologic (primarily submarine topography) data suggests that the faulting associated with this earthquake has a reverse dip-slip component of 2 m, and a right-lateral strike-slip component of 6 m. The fault plane is 130 km long and 65 km wide, and dips 45° towards $N45^\circ E$. The fault dimension and the geometry agree with the present results reasonably well in view of the various simplifications made in interpreting both the seismological and the geodetic data. However, the average dislocation on the fault plane significantly differs between these two independent studies; the seismological data suggest a displacement of about 2 m and the geodetic

data, about 7 m. One possible explanation for this discrepancy may be provided by introducing different time-constants for the displacements associated with the seismic wave radiation and the geodetic deformation; deformations having a time constant longer than several minutes would not have contributed to the generation of seismic waves. In contrast, the geodetic data represent a deformation integrated over a long period of time, some 30 years or so. The geodetic data may also include a precursory deformation that may have taken place just before the earthquake. The precursory event associated with this earthquake was discussed in detail by *Imamura* (1930). *Imamura* believed that a significant pre-seismic tilting was registered at Tokyo with an Omori clinograph which showed a sharp westward tilt during 8 hours preceding the earthquake (*Imamura*, 1928). No mareographic records, however, showed any preseismic upheaval or subsidence. Thus, although the discrepancy between the displacements estimated from the seismological and the geodetic data suggests a precursory displacement having a time-constant longer than several minutes, the evidence from other observations is not very firm.

The slip vector of the foot-wall side is almost perpendicular to the trend of the Japan trench as shown in Figure 5; the strike of the fault plane is more or less parallel to the strike of the Sagami trough. Thus this earthquake can be considered as representing a reverse right-lateral faulting on a fault plane whose surface manifestation is the Sagami trough. In view of the relatively shallow depth of this earthquake, the major fracture is considered to have occurred primarily within the crust. Since the focal region is

considerably removed from the trench, this earthquake is unlikely to be a direct consequence of an interaction between the oceanic and the continental lithospheres. Rather, it represents a slippage caused by a secondary effect of the lithospheric interaction; the slippage took place between two crustal blocks bounded by the Sagami trough. This situation is quite different from that for other great earthquakes such as the Kuril Islands (Oct. 13, 1963), Rat Island (Feb. 4, 1965) and Alaska

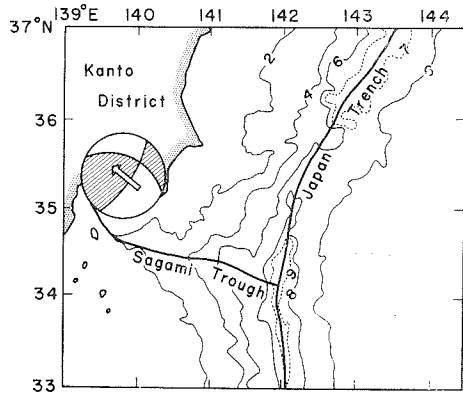


Fig. 5. Schematic mechanism diagram of the Great Kanto earthquake. The arrow shows the slip direction of the footwall side. The water depth is given in kilometers.

(March 28, 1964) earthquakes which are interpreted as a direct result of the interaction between the oceanic and the continental lithospheres (see Kanamori, 1970).

References

- ANDO, M., 1971. A fault-origin model of the Great Kanto earthquake of 1923 as deduced from geodetic data, *Bull. Earthquake Res. Inst. Tokyo Univ.*, **49**, 19-32.
- IMAMURA, A., 1928. On the tiltings of the earth preceding the Kanto earthquake of 1923, *Proceedings of the Imperial Academy of Japan*, **4**, 148-150
- IMAMURA, A., and K. HASEGAWA, 1928. List of the after-shocks of the great Kwanto earthquake, *Bulletin of the Imperial Earthquake Investigation Committee*, **11**, 64-92.
- IMAMURA, A., 1930. Topographical changes accompanying earthquakes or volcanic eruptions, *Publications of the Earthquake Investigation Committee in Foreign Languages*, No. 25, 1-143.
- KANAMORI, H., 1970. Great earthquakes at island arcs and lithosphere, to be submitted to *Tectonophysics*.
- KANAMORI, H., and S. MIYAMURA, 1970. Seismometrical re-evaluation of the great Kanto earthquake of September 1, 1923, *Bull. Earthquake Res. Inst. Tokyo Univ.*, **48**, 115-125.
- KANAMORI, H., 1971. Seismological evidence for a lithospheric normal faulting: The Sanriku earthquake of 1933, *Phys. Earth Planet. Interiors*, **4**, 289-300.
- NAKAMURA, S., 1925. On the earthquake occurred in the bay of Sagami and destroyed Tokyo, Yokohama and their vicinities on September 1st, 1923, *The Seismological Bulletin of the Central Meteorological Observatory of Japan*, **1**, 1-66.

2. 関東地震 (1923 年) の断層モデル

地震研究所 金森博雄

関東地震の断層パラメーターを P 波の初動分布と長周期表面波の振幅からきめた。その結果、この地震は $N20^{\circ}E$ の方向に 34° 傾いた面上での右ずれ・逆断層であらわされることがわかった。断層面の大きさを $130 \times 70 \text{ km}^2$ とすると、断層面上でのすべりは約 2 m 、stress drop は 18 バールである。断層上でのすべりのむきが相模 trough の走向に平行で、日本海溝に垂直であり、また震源が浅く (地殻内) かつ日本海溝から遠くはなれていることを考えると、関東地震は海と陸のリソスフィアの相互作用の直接の結果とは考えにくい。むしろ、この地震は海と陸のリソスフィアの相互作用によつて 2 次的に起つた、相模 trough を境とする二つの地塊のずれによるものであると解釈できる。地殻変動の大きさから推定されているすべりの大きさは 7 m であるが、これは表面波の振幅から推定された値 2 m よりはるかに大きい。この違いは種々の誤差を考慮にいれてもなお有意義と思われる。このくいちがいは、全体の地殻変動量のうち 2 分以内の時定数をもつもののみが地震波の発生に関与したと考えれば説明できる。